Available online at www.sciencedirect.com

SCIENCE DIRECT®

Journal of Catalysis 231 (2005) 245–253

JOURNAL OF CATALYSIS

www.elsevier.com/locate/jcat

Catalytic performance and elution of Pd in the Heck reaction over zeolite-supported Pd cluster catalyst

Kazu Okumura *, Kumiko Nota, Keiko Yoshida, Miki Niwa

Department of Materials Science, Faculty of Engineering, Tottori University, Koyama-cho, Tottori 680-8552, Japan

Received 5 November 2004; revised 17 December 2004; accepted 22 December 2004

Abstract

The Heck reaction was carried out in N,N-dimethylacetamide (DMAc) solvent with Pd-supported zeolites as catalysts. Particular attention was paid to the influence of pretreatment conditions and the kind of zeolites on the catalytic activity and the elution of Pd. Pd^{2+} ion-exchanged zeolites exhibited relatively high activity in the reaction. However, a considerable amount of Pd was dissolved in the solvent. Deposition of agglomerated Pd^0 was observed after the reaction, suggesting the dissolved Pd^{2+} species was reduced with DMAc during reaction. Pd^0-loaded zeolites were prepared by the reduction of Pd oxide/zeolites with H_2. Among Pd^0-loaded catalysts, Pd^0/H–Y exhibited high activity. The dissolution of Pd was significantly suppressed over Pd^0/H–Y, as indicated by ICP analysis of the solution. The recycled use of Pd^0/H–Y was possible through oxidation and successive reduction with H_2. The growing process of Pd clusters in H–Y was followed by energy-dispersive XAFS (partly Quick XAFS) during temperature-programmed reduction in diluted H_2. It was found that stable Pd_{13} clusters that interacted with Brønsted acid sites were generated in the pore of H–Y. The Pd_{13} clusters were ascribed to the active and insoluble species in the Heck reaction.

Keywords: Heck reaction; Palladium; EXAFS; Y-Type zeolite; Cluster

1. Introduction

Recently, much effort has been devoted to developing active Pd catalysts in the Heck reaction, because the reaction is useful and versatile for the formation of C–C bonds via the arylation or vinylation of olefins [1–3]. Furthermore, the reaction proceeds under mild conditions to yield alkylated products with high efficiency. Many kind of materials, including active carbon, metal oxides, molecular sieves, and polymeric materials, have been used as supports for heterogeneous Pd catalysts [4–7]. In these investigations, active catalysts that showed limited dissolution of Pd were desired, in view of the separation and the recycled use of catalysts. However, it has often been difficult to suppress the dissolution of Pd, and sometimes the dissolved Pd was considered to be the active species in the reaction. Arai et al. claimed that the dissolved Pd acted as active sites for the Heck reaction, which reprecipitated on active carbon supports after the reaction [8]. Djakovitch and co-workers also pointed out that Heck reaction took place on the dissolved Pd, and the dehalogenation proceeded over solid Pd catalyst [9]. Furthermore, Köhler et al. reported the highly active Pd/MO_x catalysts in the reaction with the nonactivated aryl chlorides [10]. They revealed that the highly active Pd species were generated by dissolution of Pd from the support. Zeolites and mesoporous materials have an advantageous character as supports for Pd over simple metal oxides or active carbon, in that they possess micropores or mesopores where Pd^0 clusters are encapsulated. Indeed, Djakovitch et al. studied a series of Pd-supported Na–Y zeolites prepared by the ion-exchange method, and they obtained active catalyst in the reaction between aryl bromides and olefins [11]. Jacobs and co-workers also reported that Pd-loaded mordenite was active and truly insoluble in the Heck reaction in toluene [12]. Basic zeolites, namely K^+- and Cs^+-exchanged X zeolite containing $PdCl_2$, were used as catalysts for a reaction be-

---

* Corresponding author. Fax: 81 857 31 5684.
E-mail address: okmr@chem.tottori-u.ac.jp (K. Okumura).

0021-9517/$ – see front matter © 2005 Published by Elsevier Inc.
doi:10.1016/j.jcat.2004.12.023

tween PhI or PhBr with styrene [13]. As for mesoporous materials, Ying et al. reported a highly active Pd-loaded Nb-MCM-41 catalyst prepared through the deposition of Pd complex in the vapor phase [14,15].

From systematic investigations of the behavior of Pd interacting with a zeolite support, it has been revealed that not only homogeneous pores but the presence of Brønsted acid sites played important roles in the generation and stabilization of well-dispersed metal Pd. We have obtained various metal Pd clusters in the acid-form zeolites [16]. That is, Pd_6 clusters were generated in the pores of MFI and MOR zeolites, and Pd_{13} clusters were obtained in FAU-type zeolites (H–Y and USY). The Pd clusters were reversibly generated upon simple oxidation and subsequent reduction treatment, which was achieved via the spontaneous dispersion of PdO on the acid sites of zeolites [17,18]. This observation suggested that the recovery of catalysts would be possible simply by oxidation at elevated temperature and subsequent reduction with H_2. In contrast to the H-form zeolites, metal Pd was readily agglomerated over Na–MFI that had no acid sites, indicating that the presence of Brønsted acidity was required to keep the dispersed form of metal Pd. The behavior of Pd was directly proved by means of in situ measurement of energy-dispersive XAFS (DXAFS) and Quick XAFS (QXAFS). These techniques are powerful tools for the study of dynamic structural changes in metals with a high dispersion [19]. With the use of DXAFS and QXAFS, it became possible to measure precisely the structure of metals within a few seconds to minutes. The present Pd/zeolites in particular seem to be suitable for investigation with DXAFS and QXAFS, since diluted Pd is homogeneously dispersed in the pores of zeolites. In addition, the absorption of X-rays in the zeolite matrix is small at the energy region of the Pd K-edge (24.3 keV).

The present study focused on the application of Pd^{2+} or Pd^0 clusters encapsulated in zeolite pores to liquid-phase Heck reactions. Here the reaction was conducted between bromobenzene and styrene in the DMAc solvent to yield *trans*-stilbene and 1,1-diphenylethene (Scheme 1). The catalytic performance and dissolution of Pd were correlated with the structural EXAFS characterization measured under static conditions or in situ XAFS data collected during temperature-programmed reduction in diluted H_2. Our interest was focused in particular on Pd^0 loaded on H–Y, which showed high activity in the Heck reaction, and the insolubility of Pd in the polar solvent.

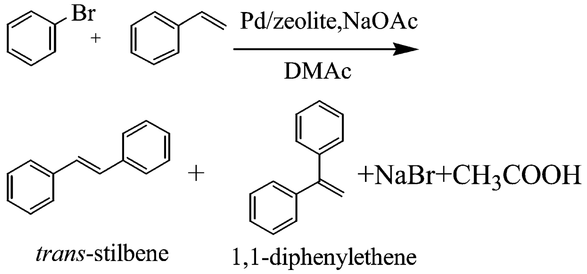

Scheme 1. Heck reaction between bromobenzene and styrene to yield *trans*-stilbene and 1,1-diphenylethene.

2. Experimental

2.1. Sample preparation

Na-, H-ZSM-5, H-mordenite, H–Y ($Si/Al_2 = 5.5$, Shokubai Kasei), USY ($Si/Al_2 = 7.51$, Shokubai Kasei), H-β ($Si/Al_2 = 25$, PQ, Co), and ferrierite ($Si/Al_2 = 17.7$, Tosoh) were used as supports for Pd. H-ZSM-5 and H-mordenite were prepared by the ion exchange of, Na-ZSM-5 ($Si/Al_2 = 23.8$, Tosoh) and Na-mordenite ($Si/Al_2 = 15$, JRC-Z-M15; Catalysis Society of Japan), respectively, with the use of NH_4NO_3 solution, followed by calcination in a N_2 flow at 723 K. Typically, Pd (0.4 wt%) was loaded on these zeolites by an ion-exchange method with the use of $Pd(NH_3)_4Cl_2$ solution at 353 K for 4 h. The samples were thoroughly washed with water and dried in air at 373 K.

2.2. Catalytic reaction and ICP analysis of dissolved Pd

Bromobenzene (10 mmol), styrene (15 mmol), and NaOAc (12 mmol) (Wako Chemicals) were used for the Heck reaction. The reaction was carried out in 10 ml of N,N-dimethylacetamide (DMAc) as solvent, which was dried over a molecular sieve. In the case of ion-exchanged ($[Pd(NH_3)_4]^{2+}$) zeolite, the sample was dried in a N_2 flow at 423 K as a pretreatment. For the preparation of the Pd^0 (metal) sample, the ion-exchanged sample was calcined in N_2, followed by oxidation with an O_2 flow at 773 K for 4 h. Finally, it was reduced with 6% H_2 diluted with Ar. In the typical condition, the Heck reaction was carried out with 0.2 g of catalyst (0.0075 mmol Pd). The batch reactor was placed in a preheated oil bath at 393 K in an atmosphere of N_2 for 4 h with stirring. After the reaction, the reaction mixture was cooled to room temperature, and then the filtered solution was analyzed with a Shimadzu 2010 Gas Chromatograph equipped with an MDN-12 (30 m) capillary column. In the analysis, DMAc (solvent) was used as an internal standard. For the recycling studies, the catalyst used in the first run was separated by filtration, and the filtered catalyst was washed with water. Then it was calcined in an O_2 flow at 773 K for 3 h to remove adsorbed organic substrates, followed by reduction with a 6% H_2 flow at 673 K.

For the measurement of the dissolved amount of Pd, the solution was filtrated, and it was evacuated on a hot plate. The residue obtained by calcination at 673 K in air was dissolved in aqua regia. The concentration of Pd was measured with the ICP method (Rigaku, Ciros).

2.3. Pd K-edge EXAFS measurement and analysis

Pd K-edge EXAFS data were collected in transmission mode at the BL10B station of Photon Factory in KEK (proposal no. 2003G289). The monochromatic X-ray beam was obtained with the use of a channel-cut Si(311) single crystal. The samples before or after the Heck reaction were pressed into wafer form. The measurement was carried out under ambient conditions.

DXAFS experiments were performed at the BL28B2 in the SPring-8 with the approval of the Japan Synchrotron Radiation Research Institute (JASRI) (proposal no. 2004A0397-NXa-np). Si polychrometer crystal was switched to a Laue configuration with a Si(422) net plane to obtain an X-ray beam with a dispersed energy region. The energy of the X-ray was calibrated with Pd foil as a reference. The sample, placed in a quartz in situ cell, was heated from room temperature to 773 K at a ramping rate of 5 $K\,min^{-1}$ in a flow of 8% H_2 diluted with He at atmospheric pressure. Total gas flow rate was 90 $ml\,min^{-1}$. Typically, spectra measured for 0.3 s were accumulated 10 times every 10 K. For the measurement of EXAFS spectra of Pd/H–Y with the lowest loading of Pd (0.2 wt%), the Quick XAFS (QXAFS) technique was applied. The experiment was carried out at the BL01B1 station in SPring-8 in a manner similar to that of DXAFS (proposal no. 2004B0311-NXa-np). The Si(111) single crystal was moved to obtain an X-ray beam with continuous energy. The time taken to collect one spectrum was 1 min.

For extended X-ray absorption fine structure (EXAFS) analysis, the oscillation was extracted from the EXAFS data by a spline smoothing method [20]. The oscillation was normalized by edge height around 50 eV above the threshold. The Fourier transformation of the k^3-weighted EXAFS oscillation from k space to r space was performed over the range of 30–150 nm^{-1} (static EXAFS data) or 30–112 nm^{-1} (DXAFS or QXAFS data) to obtain a radial distribution function. The inversely Fourier-filtered data were analyzed with a common curve-fitting method. For the curve-fitting analysis, the empirical phase shift and amplitude functions for Pd–Pd were extracted from the data for Pd foil. In the analysis of DXAFS or QXAFS spectra collected at elevated temperatures, back-scattering amplitude and phase shift were extracted from the spectra of Pd foil measured at the same temperatures. The curve-fitting analysis was initiated with the use of Debye–Waller factors extracted from EXAFS spectra of Pd foil measured at the same temperatures. The Debye–Waller factors of Pd foil at higher temperatures were determined based on the spectrum of Pd foil measured at room temperature. The certainty related to the coordination number was estimated to be 10%.

3. Results

3.1. *Catalytic performance and structural characterization of Pd^{2+}/zeolites*

Pd^{2+}/zeolite (immobilized $[Pd(NH_3)_4]^{2+}$ in zeolite) prepared from $Pd(NH_3)_4Cl_2$ with the ion-exchange method was subjected to the Heck reaction after drying in a N_2 flow at 423 K as a pretreatment. Fig. 1 gives the data of the reaction as well as the amount of Pd dissolved in DMAc. Among the tested catalysts, Pd loaded on USY, H–Y, and H-mordenite exhibited relatively high activity. However, 4.7–10.3% of Pd was dissolved from the loaded Pd. The selectivity for a yield of *trans*-stilbene (*trans*-stilbene/(*trans*-stilbene + 1,1-diphenylethene)) was 90% on these catalysts. The value was comparable to that reported by Djakovitch, who used $[Pd(NH_3)_4]^{2+}$-supported Na–Y zeolite as the catalyst [21]. The activity and the extent of the dissolution of Pd were lower over Pd/H-ZSM-5. The selectivity for *trans*-stilbene was 60% over Pd/H-ZSM-5; the value was lower than those of other catalysts. Pd^{2+} species loaded on H-ZSM-5 zeolite were probably not reduced with DMAc solvent to give Pd^0-species during the reaction; therefore the Pd^{2+}/H-ZSM-5 was inactive in the reaction.

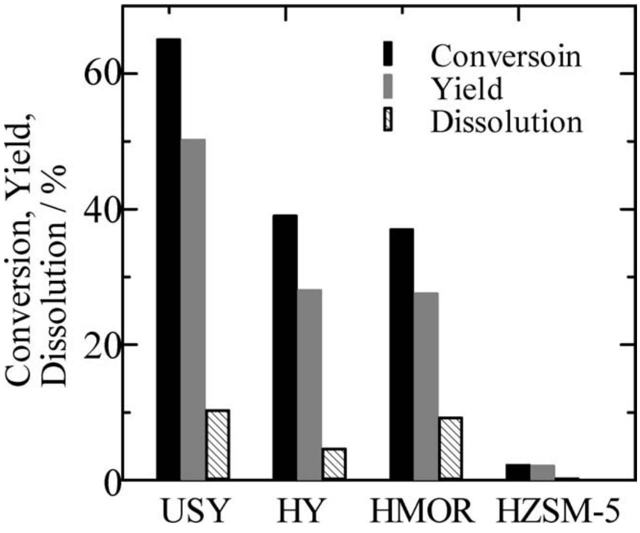

Fig. 1. Conversion of bromobenzene, yield of *trans*-stilbene and dissolution of Pd over 0.4 wt% Pd^{2+} supported zeolite catalysts. Pd, 0.0075 mmol; bromobenzene, 10 mmol; styrene, 15 mmol; NaOAc, 12 mmol; DMAc, 10 ml. Temperature, 393 K; reaction time, 4 h.

Fig. 2 gives the Fourier transforms of Pd K-edge $k^3\chi(k)$ EXAFS spectra measured before and after the reaction. For the preparation of the reacted samples, the filtered catalyst was thoroughly washed with water to remove the remaining NaBr, since it was assumed that the NaBr generated in the Heck reaction hindered the transmission of X-ray in the EXAFS measurement. In the spectra measured before reaction, a peak appeared at 0.16 nm, which could be attributed to the contribution of N in NH_3 ligand from the comparison with the spectrum of $Pd(NH_3)_4Cl_2$ as given in the figure. The intensity of the Pd–N bond decreased in the spectra of Pd/USY, HY, and H-mordenite measured after the reaction. Alternatively, a new peak appeared at 0.25 nm that could be straightforwardly assigned to the Pd–Pd bond of metal Pd. The change in the spectra indicated that the Pd^{2+} cation anchored on the ion-exchange site of zeolites was completely (USY and HY) or partially (H-mordenite) transformed to

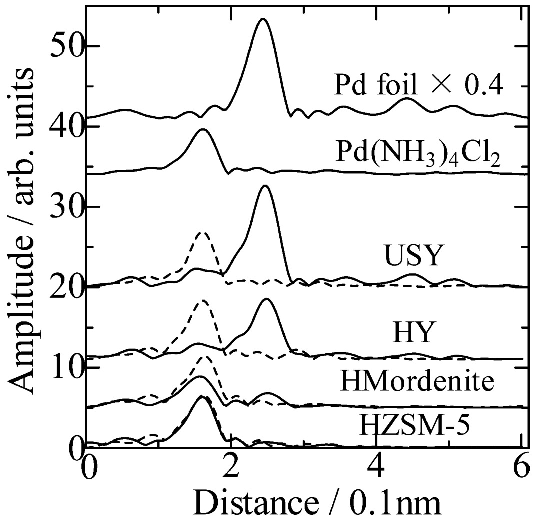

Fig. 2. Pd K-edge $k^3\chi(k)$ EXAFS Fourier transforms measured before (dotted lines) and after (solid lines) Heck reaction using 0.4 wt% Pd^{2+} supported zeolite catalysts. Fourier filtering range, 30–150 nm^{-1}.

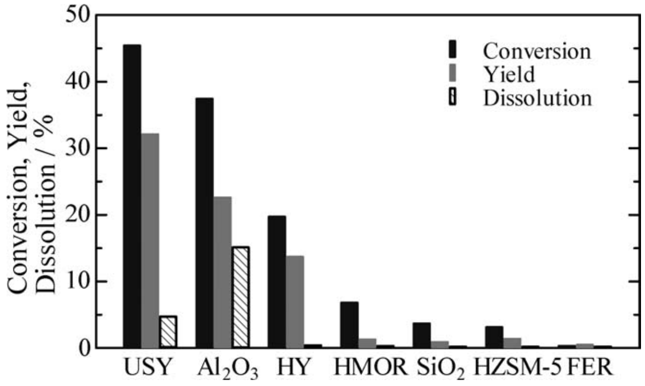

Fig. 3. Conversion of bromobenzene, yield of *trans*-stilbene and dissolution of Pd over 0.4 wt% Pd^0 supported zeolite catalysts. Pd, 0.0075 mmol; bromobenzene, 10 mmol; styrene, 15 mmol; NaOAc, 12 mmol; DMAc, 10 ml. Temperature, 393 K; reaction time, 4 h.

give metal Pd after the reaction. The change in the spectrum was not observed on Pd^{2+}/H-ZSM-5, which exhibited low activity in the reaction.

3.2. *Catalytic performance and structural characterization of Pd^0/zeolites*

Pd^0/zeolites were prepared through the calcinations of Pd^{2+}/zeolites at 773 K in a N_2 and O_2 flow, followed by reduction with 6% H_2 at 673 K. For comparison, Pd^0 loaded on Al_2O_3 and SiO_2 was prepared by the impregnation method with $Pd(NH_3)_4Cl_2$ as a precursor and subsequent reduction with H_2. Fig. 3 shows catalytic activity and dissolution of Pd over Pd^0-loaded catalysts. *trans*-Stilbene was obtained as a main product, whereas *cis*-stilbene was not detected by GC analysis in every catalyst. The selectivity for *trans*-stilbene (*trans*-stilbene/(*trans*-stilbene + 1,1-diphenylethene)) was calculated to be 90% in every catalyst. The selectivity was close to those found for Pd^{2+} catalysts. Among tested catalysts, Pd loaded on USY, HY, and Al_2O_3 exhibited relatively high activity. However, significant dissolution of Pd was observed on USY and Al_2O_3. In contrast, the dissolution of Pd was almost completely suppressed over H–Y. The insolubility of Pd in Pd^0/H–Y was confirmed by ICP analysis where the catalyst was quickly separated by filtration, until the temperature of the solution was decreased to 373 K. Such a procedure was necessary to exclude the possibility of precipitating the dissolved Pd on cooling to room temperature. The amount of dissolved Pd was analyzed to be less than 0.5% of the total Pd present in the original Pd^0/H–Y catalyst. Thus, it could be concluded that the Pd^0 on H–Y was truly insoluble in DMAc. On the other hand, Pd loaded on H-mordenite, H-ZSM-5, SiO_2, and FER exhibited lower activity, in which the conversion of bromobenzene was less than 7%.

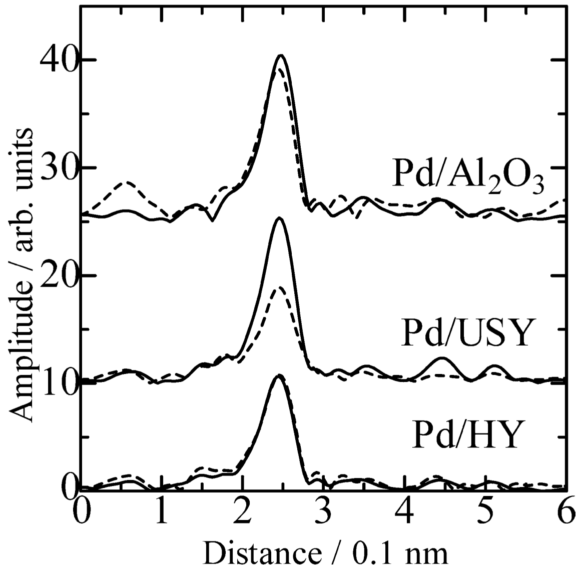

Fig. 4. Pd K-edge $k^3\chi(k)$ EXAFS Fourier transforms measured before (dotted lines) and after (solid lines) Heck reaction using 0.4 wt% Pd^0 supported zeolite and Al_2O_3 catalysts. Fourier filtering range, 30–150 nm^{-1}.

Fig. 4 gives Pd K-edge EXAFS of Pd loaded on USY, H–Y, and Al_2O_3 measured after the pretreatment with H_2 as well as after the Heck reaction. The Pd–Pd peak characteristic of metal Pd appeared at 0.25 nm in every spectrum. When USY and Al_2O_3 were used as supports for Pd, the intensity of the Pd–Pd bond of the reacted sample was higher than that of the pretreated one, indicating the agglomeration of metal Pd during reaction. The growth of Pd over USY and Al_2O_3 was probably caused by the elution of Pd into the solvent and the subsequent deposition of the metal Pd, taking into consideration that extensive dissolution of Pd was observed on these catalysts. On the other hand, the intensity of the Pd–Pd bond of the reacted sample agreed well with that of the pretreated one over Pd/H–Y. Therefore, it could be assumed that the Pd remained intact over H–Y during the course of Heck reaction, since the change in the structure of metal Pd and the dissolution of Pd were not observed on the H–Y support.

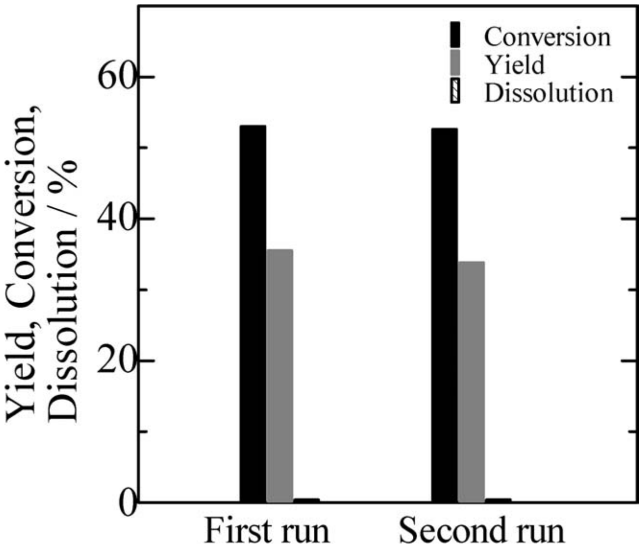

Fig. 5. Comparison of the recycle use of the Pd^0/H–Y catalyst in the Heck reaction. Temperature, 393 K; reaction time, 24 h. Pd/H–Y used in the second cycle was prepared by the oxidized with O_2 at 773 K for 3 h, followed by reduction with 6% H_2 at 673 K for 1 h after the first run.

3.3. *Recycling of Pd/H–Y catalysts*

The Heck reaction was conducted over Pd^0/H–Y for 24 h at 393 K, the filtered catalyst was washed with CH_2Cl_2, and it was used repeatedly for the Heck reaction in a manner similar to that demonstrated by Djakovitch et al. [6]. However, the catalyst was inactive in the repeated use for the reaction, probably because of the inhibition of deposited coke.

As an alternative method of regeneration, the filtered catalyst was calcined in an O_2 flow at 773 K, followed by reduction with a 6% H_2 flow at 673 K. The recovered catalyst was used repeatedly for the Heck reaction. The oxidation treatment was intended to remove the coke remaining in the catalyst. The conversion of bromobenzene, the yield of *trans*-stilbene, and dissolved Pd are compared in Fig. 5. The yield and conversion in the second run agreed with those in the first run. The dissolution of Pd was not detected in either run, as measured by ICP analysis of the filtered solution. Therefore, it was confirmed that the recycled use of Pd/H–Y was possible through oxidation with O_2 and subsequent reduction treatment with H_2.

3.4. *Influence of the pretreatment temperature on the catalytic performance*

The Heck reaction was carried out over Pd^0-loaded zeolites pretreated with a H_2 flow at different temperatures. Figs. 6 and 7 give the yield of *trans*-stilbene and the amount of dissolved Pd plotted as a function of the reduction temperature, respectively. Although the overall activity of Pd/USY was higher than those of other zeolites, 2–5% of Pd was found to dissolve in the solvent as measured by ICP analysis of filtrate. The dissolved Pd^{2+} species may be responsible for the high activity of Pd/USY, considering that the amount of dissolved Pd and the Heck reaction activity showed similar tendencies. On the other hand, the *trans*-stilbene yield was almost independent of the reduction temperature over Pd^0/H–Y, and the dissolution of Pd was negligible, especially in the reduction temperature range between 473 and 773 K. In contrast to these zeolites, Pd loaded on H-ZSM-5, H-mordenite, and ferrierite was substantially inactive in the reaction.

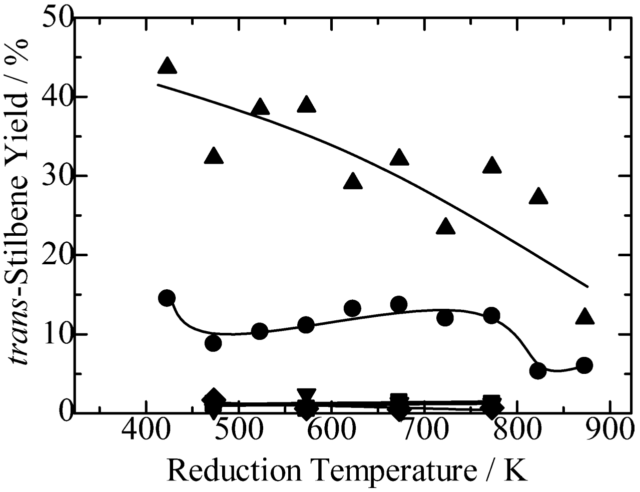

Fig. 6. Dependence of the *trans*-stilbene yield on the pretreatment temperature of 0.4 wt% Pd supported zeolite catalyst. Temperature, 393 K; reaction time, 4 h. ▲, USY; ●, H–Y; ■, H-mordenite; ▼, H-ZSM-5; ◆, ferrierite. Pd, 0.0075 mmol; bromobenzene, 10 mmol; styrene, 15 mmol; NaOAc, 12 mmol; DMAc, 10 ml. Pretreatment was carried out in 6% H_2 for 1 h.

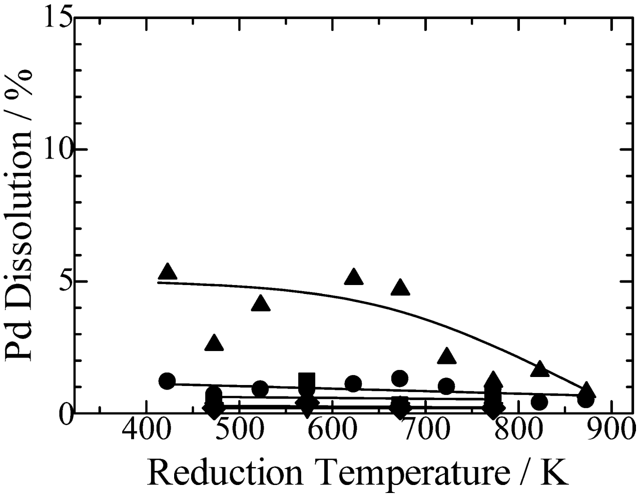

Fig. 7. Dependence of the dissolution of Pd on the pretreatment temperature of 0.4 wt% Pd supported zeolites. ▲, USY; ●, H–Y; ■, H-mordenite; ▼, H-ZSM-5; ◆, ferrierite. Pretreatment was carried out in 6% H_2 for 1 h.

3.5. *Influence of the kind of cations on the catalytic performance and elution of Pd/Y-type zeolites*

The Heck reaction was carried out over 0.4 wt% Pd loaded on Na–Y, K–Y, and Cs–Y zeolites, and the influence of the kind of cations present in the ion-exchange site of

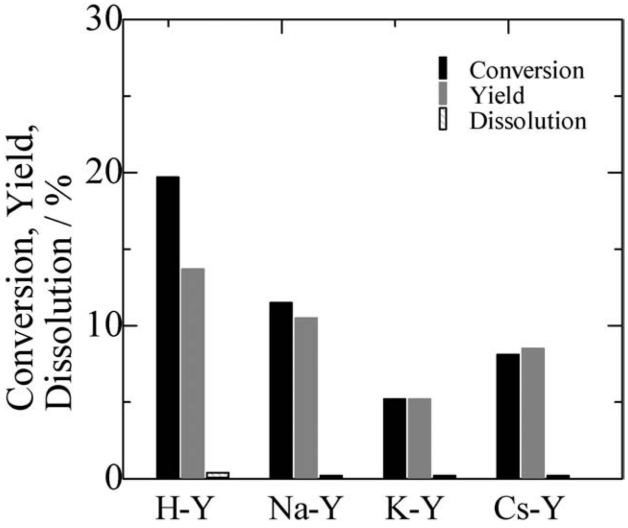

Fig. 8. Conversion of bromobenzene, yield of *trans*-stilbene and dissolution of Pd over 0.4 wt% Pd^0 supported Y-type zeolites exchanged with alkali cations. Temperature, 393 K; reaction time, 4 h.

Y-type zeolites was studied. K–Y and Cs–Y were prepared by repeated ion exchange with the use of a corresponding nitrate solution (1.4 M) and Na–Y as a starting material. Ninety-seven percent and sixty-eight percent of Na^+ ion, respectively, were ion exchanged with K^+ and Cs^+ ions as measured by ICP analysis. Before the reaction, pretreatments were undertaken at 673 K for 1 h with 6% H_2. The data of the catalytic reaction and the amount of dissolved Pd are given in Fig. 8. The conversion of bromobenzene and the yield of *trans*-stilbene over Pd-loaded cation-exchanged zeolites were lower than those obtained over Pd/H–Y. The selectivity for *trans*-stilbene was calculated to be 90% for every catalyst. The amount of dissolved Pd was less than 0.4% in every catalyst.

3.6. Heck reaction between substituted bromobenzenes and styrene over Pd/H–Y catalysts

The Heck reaction was carried out between bromobenzene derivatives and styrene to examine the effect of the activating or deactivating substituents in bromobenzene (Fig. 9). The reaction was undertaken over 0.4 wt% Pd-loaded H–Y catalysts. When bromobenzene derivatives with electron-donating substituents were used as reactants (*p*-bromotoluene and *p*-bromoanisole), the yield of products decreased in comparison with bromobenzene. In contrast, the yield increased when *p*-bromoacetophenone, with an electron-withdrawing substituent, was used as a reactant, where the conversion reached almost 100%. The tendency observed here agreed with the data given by Djakovitch and co-workers [6]. The selectivity for the *trans*-stilbene derivatives was higher than 88%. The highest selectivity (99%) was reached when *p*-bromotoluene was used as a reactant. Dissolution of Pd was not detected in DMAc in every reaction.

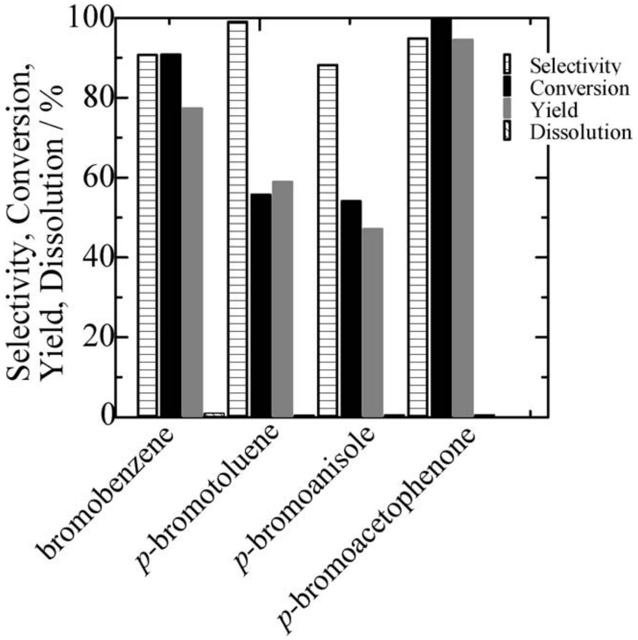

Fig. 9. Selectivity to *trans*-stilbene derivatives, conversion of bromobenzene derivatives, yield of substituted stilbenes and dissolution of Pd over 0.4 wt% Pd^0 supported H–Y zeolite. Pd, 0.0075 mmol; substituted bromobenzene, 10 mmol; styrene, 15 mmol; NaOAc, 12 mmol; DMAc, 10 ml. Reaction temperature, 413 K; reaction time, 24 h.

3.7. Growing process of Pd clusters measured by means of DXAFS and QXAFS

To reveal the role of acid sites present in the pores of H–Y, Pd was loaded on Y-type zeolites with different kinds of cations and the process of the growth of metal Pd was compared during temperature-programmed reduction with H_2. Pd K-edge DXAFS data were collected every 10 K from room temperature to 773 K at a ramping rate of 5 K min^{-1}. Representative Fourier transforms of Pd K-edge $k^3\chi(k)$ spectra of Pd(0.4 wt%)/Na–Y and Pd(0.4 wt%)/H–Y are given in Fig. 10. In the spectrum of the initial Pd/Na–Y, two peaks appeared at 0.15 and 0.32 nm, which were ascribed to the Pd–O and Pd–(O)–Pd from the comparison with bulk PdO, respectively. The appearance of the Pd–(O)–Pd bond suggested the formation of agglomerated PdO on Na–Y, because the peak was characteristic of bulky PdO. On the other hand, the Pd–(O)–Pd bond was not observed in the spectrum of Pd/H–Y, indicating the generation of highly dispersed PdO (oxide) on the acid sites of H–Y. Accompanied by a rise in the temperature, the Pd–O or Pd–(O)–Pd peaks disappeared around 373–403 K. A new peak emerged at 0.26 nm because of the formation of metal Pd. The coordination number (CN) of the nearest-neighbor Pd–Pd bond of metal Pd was calculated based on the curve-fitting analysis; the data are summarized in Fig. 11. In the case of Pd/H–Y(0.4 wt%), the CN(Pd–Pd) of metal Pd increased in the temperature range between 380 and 500 K as a consequence of the progress of the reduction of PdO to give metal Pd. Then the CN(Pd–Pd) came to the constant value at 5.5 (500–680 K).

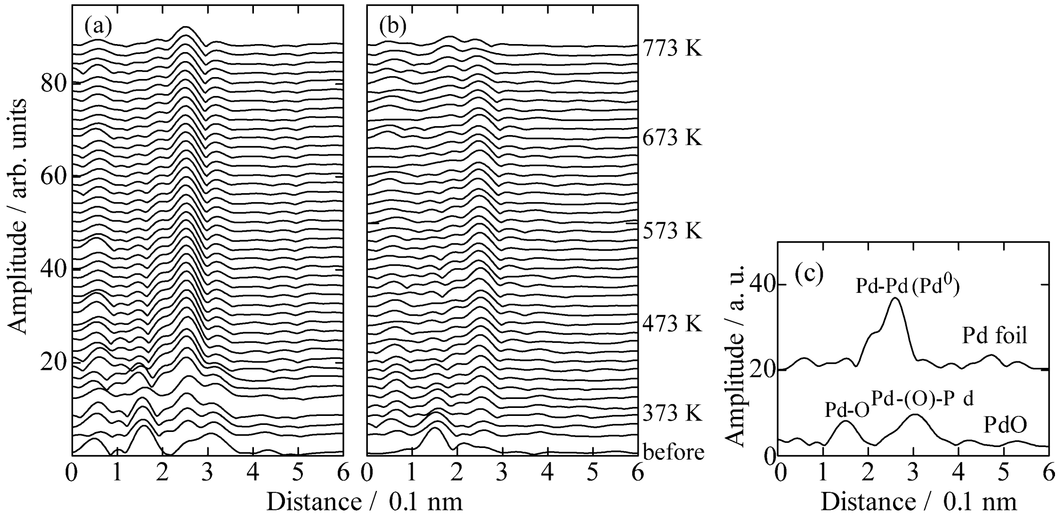

Fig. 10. Pd K-edge $k^3\chi(k)$ Fourier transforms of 0.4 wt% Pd loaded on (a) Na–Y and (b) H–Y zeolites measured during temperature programmed reduction in 8% H_2 by means of energy-dispersive XAFS method. Spectra of Pd foil and bulk PdO were measured at room temperature.

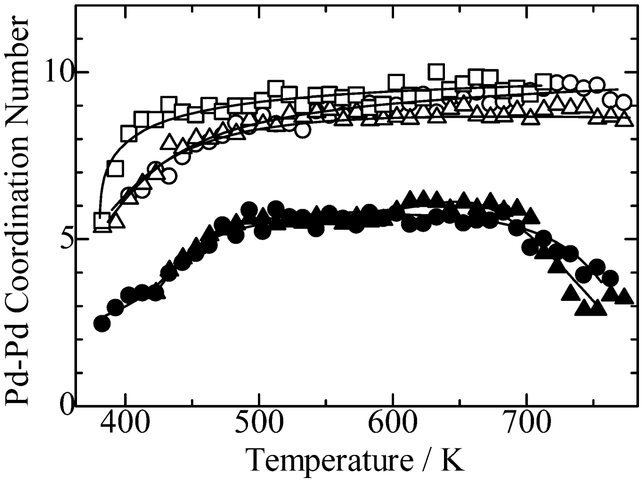

Fig. 11. Pd–Pd (metal) coordination numbers of Pd plotted as a function of temperature in the DXAFS (●, ○, △, □) or QXAFS (▲) measurement; (●) Pd(0.4 wt%)/H–Y, (▲) Pd(0.2 wt%)/H–Y, (○) Pd(0.4 wt%)/Na–Y, (△)/Pd(0.4 wt%)/K–Y and (□) Pd(0.4 wt%)/Cs–Y.

The CN observed in H–Y was in good agreement with that of clusters with a cuboctahedron (CN(Pd–Pd) = 5.5) structure composed of 13 Pd atoms. Therefore, the selective formation of stable Pd_{13} clusters located inside the supercage of H–Y was inferred from the DXAFS data. The formation of the Pd cluster was probably closely related to the catalytic performance and the insolubility of Pd. Judging from the CN, the size of the Pd_{13} cluster generated in H–Y was estimated to be 0.7 nm, assuming the cuboctahedron structure. Apparently the size was smaller than that of the diameter (1.3 nm) of the supercage in H–Y. Thus it could be thought that the Heck reaction took place in the void of the supercage adjacent to Pd clusters generated inside the supercage of H–Y. With a further rise in the temperature above 680 K, the CN began to decrease. The change was supposed to be result from the dispersion of Pd into the sodalite cage or hexagonal prism of the FAU structure [16]. A similar change in CN was observed over Pd/H–Y with a lower loading of Pd (Fig. 11, Pd 0.2 wt%). The similarity in the behavior of CN suggested that Pd clusters were homogeneously distributed over H–Y when the Pd loading was less than 0.4 wt%.

In contrast, the CN of Pd–Pd continued to increase up to 9–10 over Y-zeolite ion-exchanged with alkali cations. The change in CN indicated that the growth of metal Pd particles progressed continuously without the formation of stable Pd clusters. In view of the CN, the size of the Pd particles was estimated to be 1.6–2.4 nm, indicating that the growing of Pd progressed on the external surface of alkali cation-exchanged Y zeolite. The facile growth of the Pd was probably caused by the absence of acid sites in these zeolites, which was necessary to keep the dispersed form of Pd clusters as observed in H–Y. From the difference in the manner of growth of metal Pd, it was noticed that the presence of H^+ was required to keep the stable Pd_{13} clusters inside the pores of Y-type zeolites.

Then the growth process of metal Pd loaded on USY, H–Y zeolite, and Al_2O_3 was compared. Pd^0 loaded on these supports exhibited relatively high activity among tested samples, as already mentioned. The CNs of the nearest-neighbor Pd–Pd bond of Pd loaded on these supports are plotted as a function of the temperature in Fig. 12. As can be seen from the figure, the change of CN in Pd/USY was similar to that of Pd/H–Y. In the case of Pd/Al_2O_3, the CN reached 7.0 after the initial reduction of PdO. The value was higher than that of Pd/H–Y or USY, implying the formation of larger metal Pd particles on the Al_2O_3 support.

4. Discussion

From comparative experiments using Pd-loaded zeolites, it was revealed that various factors, including support materials and pretreatment conditions, influenced the catalytic performance and the solubility of Pd. The reason for this

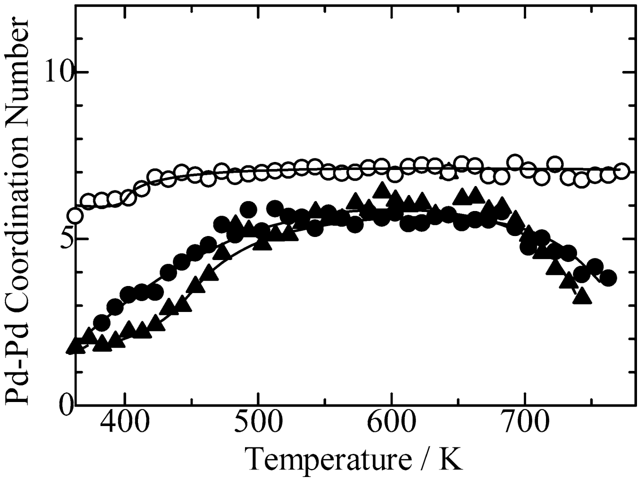

Fig. 12. Pd–Pd (metal) coordination numbers of Pd loaded on (●) H–Y, (▲) USY, and (○) Al_2O_3 plotted as a function of reduction temperature in the DXAFS measurement.

was closely related to the valence state of Pd and the formation of Pd clusters. Pd^{2+} cations exhibited higher activity in comparison with Pd^0 produced by the reduction with H_2. However, significant dissolution of Pd was observed when Pd^{2+}-loaded zeolites were used as catalysts, except for Pd^{2+}/H-ZSM-5, which was inactive in the reaction. In the active catalysts, Pd^{2+} present in zeolites was reduced to give Pd^0 after the reaction, as indicated by EXAFS measurements. The change in Pd suggested that the dissolution and re-precipitation took place in the course of the catalytic reaction. Taking these observations into consideration, it was supposed that the dissolved Pd^{2+} was responsible for the high activity of Pd^{2+}/zeolites. These facts seemed to contradict the report by Jacobs et al., who used toluene as a solvent [22]. They reported that $Pd(NH_3)_4{}^{2+}$-mordenite exhibited activity in the Heck reaction and the Pd^{2+} cation was truly insoluble in toluene. In contrast with their observation, 9.2% loaded Pd was dissolved from Pd/H-mordenite in our experiment (Fig. 1). The difference in the kind of solvent was assumed to be the reason for the contradictory results. That is to say, DMAc used in the present experiment has a much more polar character compared with toluene. Therefore, it could be supposed that DMAc promoted the dissolution of Pd^{2+} in DMAc solvent over mordenite.

Among Pd^0/zeolites, Pd loaded on H–Y and USY with the FAU-type structure exhibited high activity in the reaction. The most striking result is that the elution of Pd was significantly suppressed over Pd/H–Y. In agreement with the insolubility of Pd in H–Y, the structure of Pd^0 was completely preserved during reaction, as indicated by Pd K-edge EXAFS (Fig. 4). In addition, the regeneration of Pd/H–Y catalyst was possible simply by oxidation and repeated reduction treatments. From the DXAFS (partially QXAFS) measurement carried out during temperature-programmed reduction in a H_2 atmosphere, the generation of stable Pd_{13} clusters was observed on H–Y. We supposed that the Pd_{13} cluster was the active species in the Heck reaction. Two possibilities could be proposed to explain the effect of the supercage of FAU zeolite on the formation and catalysis of Pd_{13} clusters. One is the steric confinement of the Pd_{13} cluster in the supercage of H–Y. However, this does not seem to be the case, when we consider that the size of the Pd_{13} cluster was smaller than the pore size of the supercage, as already mentioned in Section 3.7. The other hypothesis is that the Pd_{13} cluster was anchored on the Brønsted acid sites. In agreement with this hypothesis, Y-type zeolites ion-exchanged with alkali cations could not keep the dispersed Pd clusters because of the lack of acid character. Similarly, Sachtler et al. proposed the proton–metal adduct “PdH^+” in the studies of Pd-supported H-form ZSM-5 [23,24]. The reason for the difference in the catalytic performance and solubility of Pd between Pd/H–Y and Pd/USY was not clearly understood at this stage, considering that similar Pd clusters were generated on the two zeolites.

5. Conclusions

The influence of the pretreatment conditions, kinds of support on the catalytic performance, and elution of Pd were studied over Pd loaded on various kinds of zeolites in the Heck reaction. Pd^{2+}-loaded zeolites exhibited relatively high activity in the reaction. These catalysts showed significant dissolution of Pd^{2+} and the deposition of Pd^0 after the reaction. Pd^0/H–Y generated by the reduction with H_2 exhibited activity in Heck reaction, whereas Pd was completely insoluble in the DMAc solvent. The reason for the superior character of Pd^0/H–Y was attributed to the formation of stable Pd_{13} clusters kept inside the supercage of H–Y, as indicated by in situ XAFS measurements.

References

[1] A. Biffins, M. Zecca, M. Basato, J. Mol. Catal. A 173 (2001) 249.

[2] K. Ferré-Filmon, L. Delaude, A. Demonceau, A.F. Noels K., Coord. Chem. Rev. 248 (2004) 2323.

[3] W.A. Herrmann, C. Brossmer, K. Öfele, C.-P. Reisinger, T. Priermeier, M. Beller, H. Fischer, Angew. Chem. 34 (1995) 1844.

[4] K. Mori, K. Yamaguchi, T. Hara, T. Mizugaki, K. Ebitani, K. Kaneda, J. Am. Chem. Soc. 124 (2002) 11572.

[5] B.M. Bhanage, M. Arai, Catal. Rev. 43 (2001) 315.

[6] L. Djakovitch, K. Koehler, J. Mol. Catal. A 142 (1999) 275.

[7] B.M. Choudary, S. Madhi, N.C. Chowdari, M.L. Kantam, B. Sreedhar, J. Am. Chem. Soc. 124 (2002) 14127.

[8] F. Zhao, K. Murakami, M. Shirai, M. Arai, J. Catal. 194 (2000) 479.

[9] L. Djakovitch, M. Wagner, C.G. Hartung, M. Beller, K. Köhler, J. Mol. Catal. A 219 (2004) 121.

[10] S.S. Pröckl, W. Kleist, M.A. Gruber, K. Köhler, Angew. Chem. Int. Ed. 43 (2004) 1881.

[11] L. Djakovitch, K. Köhler, J. Am. Chem. Soc. 123 (2001) 5990.

[12] M. Dams, L. Drijkoningen, D.D. Vos, P. Jacobs, Chem. Commun. (2002) 1062.

[13] A. Corma, H. García, A. Leyva, A. Primo, Appl. Catal. A 247 (2003) 41.

[14] C.P. Mehnert, J.Y. Ying, Chem. Commun. (1997) 2215.

[15] C.P. Mehnert, D.W. Weaver, J.Y. Ying, J. Am. Chem. Soc. 120 (1998) 12289.

[16] K. Okumura, R. Yoshimoto, T. Uruga, H. Tanida, K. Kato, S. Yokota, M. Niwa, J. Phys. Chem. B 108 (2004) 6250.

[17] K. Okumura, J. Amano, N. Yasunobu, M. Niwa, J. Phys. Chem. B 104 (2000) 1050.

[18] K. Okumura, T. Kusakabe, S. Yokota, K. Kato, H. Tanida, T. Uruga, M. Niwa, Chem. Lett. 32 (2003) 636.

[19] M.K. Neylon, C.L. Marshall, A.J. Kropf, J. Am. Chem. Soc. 124 (2002) 5457.

[20] J.B. Van Zon, D.C. Koningsberger, H.F.J. Van Blik, D.E. Sayers, J. Phys. Chem. 82 (1985) 5742.

[21] L. Djakovitch, H. Heise, K. Köhler, J. Organomet. Chem. 584 (1999) 16.

[22] M. Dams, L. Drijkoningen, B. Pauwels, G. Van Tendeloo, D.E. De Vos, P.A. Jacobs, J. Catal. 209 (2002) 225.

[23] X. Bai, W.M.H. Sachtler, J. Catal. 129 (1991) 121.

[24] S.T. Homeyer, Z. Kapinski, W.M.H. Sachtler, J. Catal. 123 (1990) 60.